ACS APPLIED ENGINEERING MATERIALS

pubs.acs.org/acsaenm Letter

Metal Ions Removal from Organic Solvents using MXene-Based Membranes

Syed Ibrahim Gnani Peer Mohamed, Ahmad Arabi Shamsabadi, Sepideh Kavousi, Mostafa Dadashi Firouzjaei, Mark Elliott, Sanaz Yazdanparast, Siamak Nejati, Mohsen Asle Zaeem, and Mona Bavarian*

Cite This: *ACS Appl. Eng. Mater.* 2023, 1, 2452–2457 Read Online

ACCESS | Metrics & More | Article Recommendations | Supporting Information

ABSTRACT: We investigated the applicability of membranes, prepared with $Ti_3C_2T_x$ MXene as the active layer, for metal ion removal from an organic solvent. The removal of various mixed metal ions from propylene glycol monomethyl ether acetate, commonly used in the microelectronics industry, was evaluated. The MXene membrane exhibited over 90% removal efficiency for metal ions such as Li, Ca, Cr, Fe, Ni, and Co and over 80% for metal ions such as Al, V, and Pb from a solution containing 17 metal ions. This result highlights the potential of MXene as an effective material for ion removal from organic solvents.

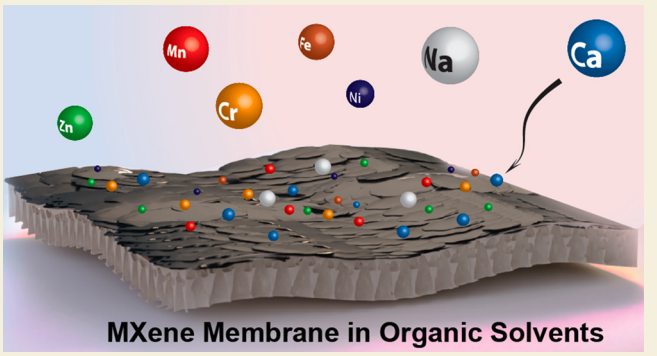

KEYWORDS: *MXene, metal ion removal, organic solvent, microelectronics, adsorptive membrane*

The constant advancement in the microelectronics (semiconductor) industry has led to the economically feasible micro- and nanofabrication of integrated circuits (ICs).[1] In the process of miniaturization of ICs, quality control is very stringent for the processing fluids; even part per billion (ppb) contaminants can lead to the failure of devices.[2,3] The main defects caused by solvents and materials used in chip manufacturing are particles and metal ions.[4,5] Although most particles can be removed by a sieving mechanism using nanofiltration membranes, the removal of trace amounts of metal ions is challenging.[6] For instance, metal ions such as Fe, Cu, Ni, Cr, Co, Pt, and Ir dissolve in the Si matrix and/or form silicide, causing p−n junction leakage.[7] Additionally, Cr contamination results in reliability degradation of the gate dielectric.[8] Furthermore, the presence of these metal ions impacts the gate oxide quality of ICs.[9] Therefore, the maximum concentration of these metallic impurities in the processing liquid should be maintained at sub ppb levels.[10,11]

In the semiconductor industry, solvents such as cyclohexanone (CHN), ethyl lactate (EL), isopropyl alcohol (IPA), *n*-butyl acetate (nBA), propylene glycol monomethyl ether acetate (PGMEA), and propylene glycol monomethyl ether (PGME) are commonly used.[12] Among these, PGMEA and PGME are predominantly used as solvents for photoresists and antireflective coatings. To purify these solvents, technologies such as ion exchange,[13] reactive distillation,[14] liquid−liquid extraction,[15] adsorption,[16] and membrane separation[17] are presently employed. Among these technologies, membrane-based separation was found to present fewer operational challenges. For instance, compared with energy-intensive processes such as distillation and extraction, membrane-based separation is an easy process with less energy demand. To date, different polymeric membranes such as nylon, polyethylene, and polypropylene were used for the removal of various metal ions from PGMEA.[17] Among the membranes tested, the nylon-based membranes exhibited higher removal efficiency for both trivalent and divalent metal ions; however, the membrane exhibited low removal efficiency toward the monovalent metal ions.[17] Hence, media with excellent metal removal efficiency and high sorption capacity are still in high demand.

Recently, an increased amount of interest has been shown in the use of two-dimensional (2D) materials as adsorbents.[18] MXenes are a relatively young class of 2D transition metal carbides, carbonitrides, and nitrides, which are analogous to graphene.[19] They are prepared by selective etching of layers of atoms such as aluminum (Al), silicon (Si), and gallium (Ga) from hexagonal MAX phases, where M is an early transition metal, A signifies an A-group (mostly IIIA and IVA, or groups

Received: August 7, 2023
Revised: September 11, 2023
Accepted: September 15, 2023
Published: October 11, 2023

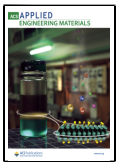

https://doi.org/10.1021/acsaenm.3c00450
ACS Appl. Eng. Mater. 2023, 1, 2452−2457

13 and 14) element, and X stands for carbon and/or nitrogen.[19]

The efficacy of MXene-based films in removing metal ions from aqueous solutions has been explored.[20] The obtained results indicated that the −OH groups on MXenes improve the film's wettability and enhance the adsorption capacity. High removal efficiencies of heavy metal ions such as Pb from wastewater using MXene were achieved.[18] The high metal removal capacity of MXene was attributed to the contribution of different mechanisms and intermolecular forces such as electrostatic attractions, ion exchange, and surface complexation.[21] It is also reported that the cationic metal ions, depending on their size and charge, can intercalate between the layers of MXenes.[22]

Herein, we report the effective removal of ions from organic solution using $Ti_3C_2T_x$ MXene (T_x: surface termination) coated on high-density polyethylene (HDPE). The prepared media functions as an adsorptive membrane in removing metal ions from PGMEA. The adsorption of metal ions on MXene-based membranes submerged in the organic solvent containing mixed metal ions is investigated. First-principles calculations reveal a favorable adsorption energy for ions on MXene nanosheets, providing insights into the strength of MXene−ion interactions.

The schematic of the MXene membrane preparation is shown in Figure 1. The details of MXene synthesis and fabrication of the MXene membrane are given in Supporting Information (SI), section 1. Briefly, the MAX phase (Ti_3AlC_2) was treated with a hydrofluoric acid (HF) solution to etch the Al layers, followed by dimethyl sulfoxide (DMSO) intercalation to obtain MXene with expanded nanochannels. Metal contaminants were removed from the HDPE substrate by soaking the substrate in a 5% aqueous hydrochloric acid (HCl) solution for 24 h, followed by deionized water washing. Subsequently, a MXene membrane was formed on the HDPE substrate by vacuum-assisted filtration of MXene from a colloidal solution. The substrates made of HDPE, a prevalent polymer, and MXene demonstrate favorable compatibility owing to their relatively modest surface energies. Additionally, the possibility of establishing hydrogen bonding between MXene and HDPE, facilitated by the oxygen (O) groups in MXene and the hydrogen (H) moieties in HDPE, opens up the prospect of creating durable membranes.[23] The top surface scanning electron microscopy (SEM) image of the MXene membrane is shown in Figure 1B, verifying the excellent coverage of the HDPE substrate with the MXene nanoflakes. The presence of a wrinkled surface, visible from top-down SEM, indicates stacking of flexible nanosheets. The cross-sectional SEM image of the MXene membrane is depicted in Figure 1C and shows the typical oriented lamellar structure. Furthermore, restacking of a few layers was observed due to the intersheet interaction. The thickness of the MXene layer on HDPE was controlled at 1.0 μm. The lamellar structure of the MXene membrane was further characterized by powder X-ray diffraction (PXRD). Supporting Information (SI), Figure S1 shows the PXRD patterns of Ti_3AlC_2 MAX powder and the $Ti_3C_2T_x$ MXene membrane. The shift of the (002) peak to lower 2θ and disappearance of the intense peak at 2θ of 39° indicate the conversion of Ti_3AlC_2 into $Ti_3C_2T_x$ MXene.[24] The X-ray photoelectron spectroscopy (XPS) (SI, Figure S2) indicated that the as-prepared MXene membrane surface is terminated with -O, −OH, and −F functional groups, which is in alignment with the reported data in the literature.[25] Furthermore, the nitrogen adsorption−desorption isotherm, depicted in SI, Figure S3, was utilized to assess both the Brunauer−Emmett−Teller (BET) surface area and the pore size distribution of MXene. This isotherm exhibits a type IV adsorption isotherm, featuring a H3 hysteresis loop. The specific surface area of the MXene layer is estimated to be 12.5 $m^2\ g^{-1}$. As shown in SI, Figure S3, the distinct hysteresis loop in between the adsorption and desorption branches within the relative pressure range of 0.45 to 1.0 for MXene is an indication of the mesoporous structure of the MXene layer. Additionally, the nearly vertical tails observed near the relative pressure of 1.0 indicate the existence of macropores.

To remove any metal contamination during membrane fabrication, the MXene/HDPE membranes were cleaned with a 5% aqueous HCl solution, followed by washing the membranes several times with deionized water. The acid-washed MXene membrane was used for removing metal ions from a mixture of 17 mixed metal ions in PGMEA. The experiment was performed under pressure-free conditions by submerging the substrate in the challenge solution at ambient temperature. The details of sample preparation and experimental methods are available in the SI, section 1. As presented in Figure 2A, the MXene membrane exhibited superior removal efficiency for various monovalent, divalent, and multivalent ions such as Li, Mg, Al, Ca, V, Cr, Na, K, Fe, Ni, Cu, Mn, Co, Zn, Cd, Ba, and Pb ions when compared with the pristine HDPE membrane. The metal ions such as Li, Mg, Ca, Cr, Fe, Ni, Cu, Mn, and Co were removed above 90%, and metal removal efficiencies of above 80% were achieved for Al,

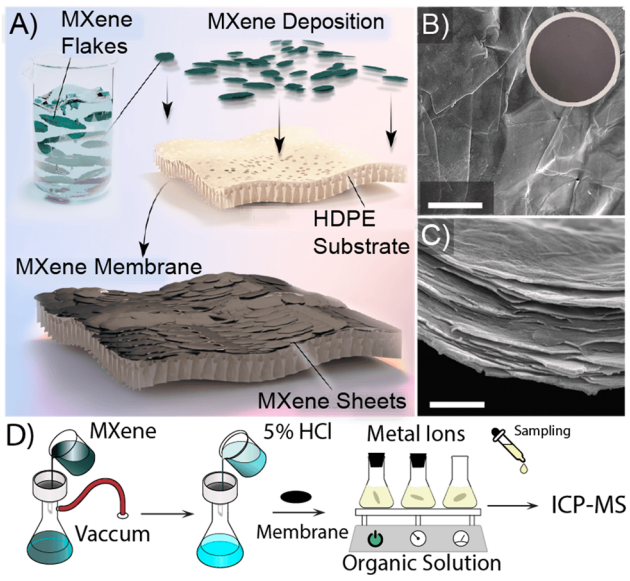

Figure 1. Preparation and microscopic analysis of the MXene membrane: (A) Schematic of MXene membrane preparation, here MXene suspension in water was vacuum filtered through a highly porous support made of high-density polyethylene (HDPE) to construct a MXene film on the HDPE surface. (B,C) top surface and cross-sectional SEM images of the MXene membrane, respectively. (D) Schematic representation of the steps taken to prepare samples and test them for metal ion removal from a mixture of 17 mixed metal ions in PGMEA. The inset in (B) shows the digital photographic image of the as-prepared MXene/HDPE membrane. The MXene membrane was prepared by filtering around 5 mg of MXene via vacuum-assisted filtration on the HDPE support at room temperature.

https://doi.org/10.1021/acsaenm.3c00450
ACS Appl. Eng. Mater. 2023, 1, 2452−2457

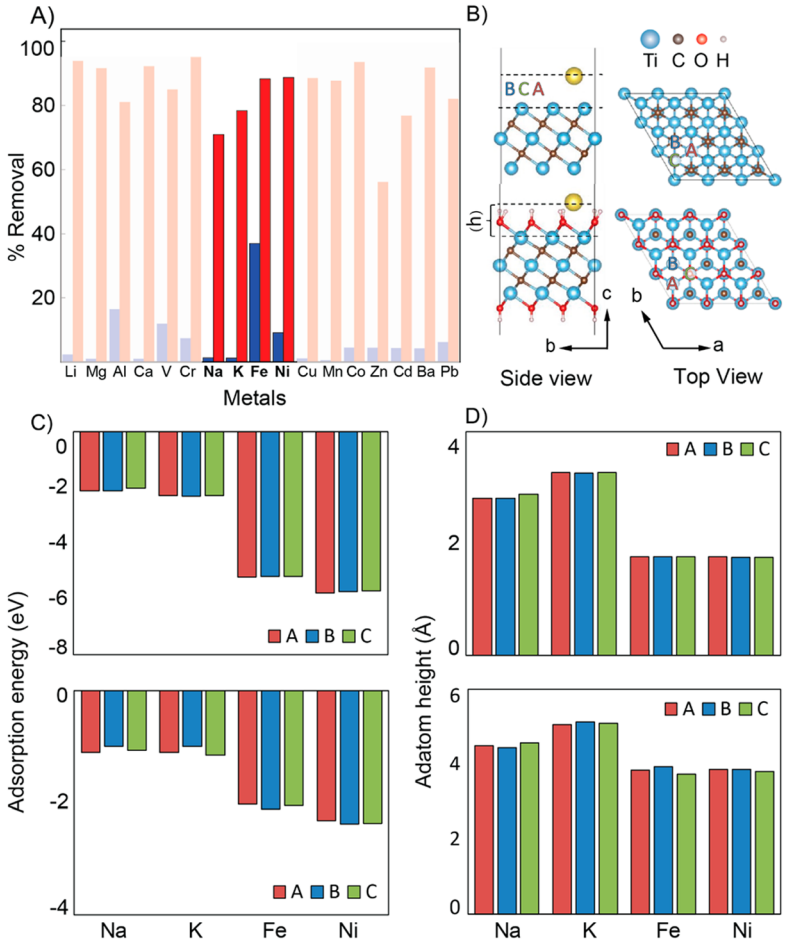

Figure 2. Ion removal and interaction with MXene-coated membranes: (A) Metal ion removal efficiency of the control HDPE (blue bar) and MXene/HDPE (red bar) membranes. The metal adsorption was performed with 100 ppb of mixed metal ions in PGMEA at 22 °C. The membrane was immersed into the test solution and kept under shaking (120 rpm) for 24 h at 22 °C to reach equilibrium. (B) Schematic diagram showing the crystal structure of Ti_3C_2 (top) and $Ti_3C_2(OH)_2$ (bottom) monolayers with side and top views (h represents the adatom height). (C,D) Adsorption energies and adatom height of Na, K, Fe, and Ni atoms on Ti_3C_2 (top) and $Ti_3C_2(OH)_2$ (bottom) monolayer. Here, red, green, and blue bars refer to the adsorption sites on the MXene nanosheet as labeled in (B).

V, and Pb ions. Among the metal ions studied, ions such as Na, K, Fe, and Ni are mostly encountered in the solvents used in the microelectronics industry and their removal is challenging.[6] As shown in Figure 2A, the metal ions such as Fe and Ni ions were removed more efficiently compared with monovalent ions such as K and Na ions. The higher removal efficiency of Fe and Ni ions can be attributed to the higher electrostatic attraction between MXene and divalent/multivalent ions compared to monovalent ions. Among the monovalent ions such as Na and K, the higher removal of K ions can be attributed to its lower solvated radius when compared with Na ions; the latter facilitated the intercalation of K ions into the MXene layers.[26,27]

The interaction between MXene and different metal ions was further investigated with density functional theory (DFT) calculations. We investigated three different adsorption sites, marked as A, B, and C in Figure 2B. The A site is at the center of a hexagon composed of carbon atoms, the B site is directly above the carbon atom, and the C site is directly above the Ti atom. The adsorption energy (E_{ad}) for all four metals adsorbed on MXene is defined as

$$E_{ad} = E_{total} - E_{MXene} - E_m$$

where E_{total} is the total energy of the MXene layer with the adatom element attached, E_{MXene} is the total energy of the pristine MXene layer, and E_m is the total energy of the isolated metallic element. The negative adsorption energies presented in Figure 2C reveal that all four investigated metal ions (Na, K, Fe, and Ni ions) can be spontaneously adsorbed on the Ti_3C_2 and −OH terminated Ti_3C_2 MXene surfaces. The adsorption energies for all four elements and all three absorption sites follow the order of Ti_3C_2 > $Ti_3C_2(OH)_2$ suggesting that the bare MXene has a higher affinity for adsorbing investigated elements when compared with the −OH terminated MXene. The negative adsorption energy obtained for both cases supports the experimentally observed applicability of both bare and −OH terminated Ti_3C_2 MXene as adsorptive membranes for the removal of metal ions. As shown in Figure 2C (top graph), the adsorption energies for the alkali metal ion (Na and K ions) on the bare Ti_3C_2 were in the range of −1 to −2.3 eV. Meanwhile, the two investigated transition metal ions (Fe and Ni ions), have a much stronger adhesion on Ti_3C_2. A similar trend, given in Figure 2C (bottom graph), was observed for −OH terminated Ti_3C_2. This trend supports the experimentally observed higher removal percentages of Fe and Ni ions in comparison to Na and K ions. The adhesion

https://doi.org/10.1021/acsaenm.3c00450
ACS Appl. Eng. Mater. 2023, 1, 2452−2457

height, which is the distance between the adatom and Ti atoms, is calculated and presented in Figure 2D. The comparison of the results between the alkali and transition metal ions indicates a decrease in the adatom height as the adhesion becomes stronger.

To gain more insights into the mechanism of metal ion removal, we studied the local chemical environment of metal ions adsorbed onto the MXene/HDPE membrane using X-ray photoelectron spectroscopy (XPS). Figure 3A presents the

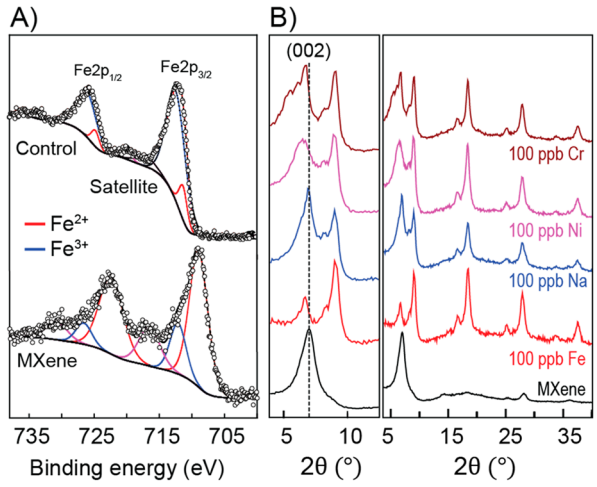

Figure 3. XPS and PXRD spectra of MXene/HDPE membranes after the adsorption of metal ions: (A) XPS high-resolution Fe 2p spectra of MXene/HDPE membranes and control HDPE membrane. (B) PXRD patterns of MXene and metal adsorbed MXene/HDPE membranes. The metal adsorption was performed with 100 ppb of each metal ion in PGMEA at 22 °C. The membrane was immersed into the test solution and kept under shaking (120 rpm) for 24 h at 22 °C to reach equilibrium.

XPS high-resolution Fe 2p spectra of the control and MXene/HDPE membranes after metal ion adsorption. Here, the control experiment was performed by submerging the HDPE membrane in the respective metal ion solution for comparison against the MXene/HDPE membrane. The peaks at 711.3 and 724.8 eV and peaks at 712.4 and 726.1 eV can be assigned to Fe^{2+} and Fe^{3+}, respectively. In the spectrum of the MXene/HDPE membrane sample, the intensity of the Fe^{3+} peak was reduced compared to Fe^{2+}, which indicates that the Fe ions are reduced upon contacting with MXene. Here, the reduction of Fe^{3+} to Fe^{2+} was assisted by the electron transfer from MXene to Fe^{3+}.[28] The zeta potential analysis of the MXene/HDPE membrane revealed that the as-prepared $Ti_3C_2T_x$ MXene membrane has an isoelectric point (IEP) of ~2.5 (SI, Figure S4).[29] Therefore, the partial negative charge of MXene (due to the presence of the −OH group) attracts positively charged metal ions. Similarly, the XPS high-resolution Cr 2p spectra exhibited the same trend. As shown in SI, Figure S5, Cr^{6+} ($Cr_2O_7^{2-}$) undergoes reduction upon contact with the MXene layer, leading to the appearance of Cr^{3+} in the XPS data (see the reduction half-reaction equation in SI, eq S2). We did not observe any shift for Na and Ni elements upon contact with MXene (SI, Figure S6), which can be attributed to the relatively lower oxidative potential of Na and Ni ions when compared to Fe and Cr ions.

The X-ray diffractograms of samples before and after the adsorption of metal ions were further used to evaluate the structural changes. As shown in Figure 3B, the (002) peak of MXene was slightly broadened and shifted to lower angles after the adsorption of different metal ions; this indicates an increase in the *d*-spacing between the MXene sheets due to the intercalation of metal ions. This shift in the position of the (002) peak was slightly smaller for monovalent ions compared to other metal ions. This can be attributed to the smaller ionic radii of the monovalent ions. We also note the appearance of a new set of peaks in the PXRD patterns of the MXene membranes upon the adsorption of metal ions, which was similar to multilayer MXene PXRD patterns.[30] Thus, we concluded that the adsorption of metal ion on MXene sheets promotes the stacking of flakes to construct multilayer MXene, for which two sets of peaks with their higher index diffraction pattern can be recorded.

This study demonstrates the tremendous potential of MXene membranes for metal ion removal from organic solvents. The reductive adsorption behavior of the MXene/HDPE membrane offered improved metal ion removal from PGMEA under pressure-free conditions. Importantly, despite the competitive adsorption of 17 metal ions, excellent removal efficiencies of >90% were obtained for Li, Mg, Ca, Cr, Fe, Ni, Cu, Mn, and Co ions. This work will open new avenues for the development of ion-selective MXene-based membranes.

■ ASSOCIATED CONTENT

Data Availability Statement

The data that support the findings of this study are available from the corresponding author upon reasonable request.

Supporting Information

The Supporting Information is available free of charge at https://pubs.acs.org/doi/10.1021/acsaenm.3c00450.

Experimental procedure, characterization, zeta potential, XPS, PXRD, and DFT calculation (PDF)

■ AUTHOR INFORMATION

Corresponding Author

Mona Bavarian − *Department of Chemical and Biomolecular Engineering, University of Nebraska−Lincoln, Lincoln, Nebraska 68588, United States;* orcid.org/0000-0001-7689-773X; Email: mona.bavarian@unl.edu

Authors

Syed Ibrahim Gnani Peer Mohamed − *Department of Chemical and Biomolecular Engineering, University of Nebraska−Lincoln, Lincoln, Nebraska 68588, United States;* orcid.org/0000-0001-9460-8620

Ahmad Arabi Shamsabadi − *Department of Chemistry, University of Pennsylvania, Philadelphia, Pennsylvania 19104, United States;* orcid.org/0000-0002-9726-2466

Sepideh Kavousi − *Department of Mechanical Engineering, Colorado School of Mines, Golden, Colorado 80401, United States*

Mostafa Dadashi Firouzjaei − *Department of Civil, Construction, and Environmental Engineering, University of Alabama, Tuscaloosa, Alabama 35487, United States;* orcid.org/0000-0002-0215-8210

Mark Elliott − *Department of Civil, Construction, and Environmental Engineering, University of Alabama, Tuscaloosa, Alabama 35487, United States;* orcid.org/0000-0002-7835-0612

https://doi.org/10.1021/acsaenm.3c00450
ACS Appl. Eng. Mater. 2023, 1, 2452−2457

Sanaz Yazdanparast − *Intel Corporation, Chandler, Arizona 85226, United States*
Siamak Nejati − *Department of Chemical and Biomolecular Engineering, University of Nebraska−Lincoln, Lincoln, Nebraska 68588, United States;* orcid.org/0000-0002-1807-2796
Mohsen Asle Zaeem − *Department of Mechanical Engineering, Colorado School of Mines, Golden, Colorado 80401, United States;* orcid.org/0000-0002-5164-6122

Complete contact information is available at: https://pubs.acs.org/10.1021/acsaenm.3c00450

Author Contributions

All authors have read and approved the final manuscript. SIGP. Mohamed, S. Nejati, A. A. Shamsabadi and M. Bavarian envisioned and conceptualized. SIGP. Mohamed, S. Nejati, A. A. Shamsabadi and M. Bavarian envisioned the study design and took part in data collection and analysis. S. Kavousi and M. Asle Zaeem took part in DFT studies. SIGP. Mohamed, S. Kavousi, M. D. Firouzjaei, drafted the manuscript. A. A. Shamsabadi, S. Yazdanparast, M. Asle Zaeem, M. Elliott, S. Nejati, and M. Bavarian revised the manuscript.

Notes

The authors declare no competing financial interest.

■ ACKNOWLEDGMENTS

M. Bavarian acknowledges the support of the National Science Foundation (NSF) under the Award Number 2238147. The research was performed in part in the Nebraska Nanoscale Facility: National Nanotechnology Coordinated Infrastructure and the Nebraska Center for Materials and Nanoscience, which are supported by the National Science Foundation under Award ECCS: 1542182, and the Nebraska Research Initiative. S. Kavousi and M. Asle Zaeem are grateful for the supercomputing time allocation provided by the NSF ACCESS (Advanced Cyberinfrastructure Coordination Ecosystem: Services & Support), Award No. TG-DMR140008.

■ REFERENCES

(1) Winkler, E. M.; van Swaay, M. An Introduction to Microelectronics. *J. Chem. Educ.* **1973**, *50* (6), A325.
(2) Baltzinger, J.-L.; Delahaye, B. Contamination Monitoring and Analysis in Semiconductor Manufacturing. *Semicond Technol.* **2010**, *2010*, 57−78.
(3) Umeda, T.; Tsuzuki, S. Defect Precursor and Metal Reduction from DSAL Resist Using Filtration and Ion Exchange. *J. Photopolym. Sci. Technol.* **2014**, *27* (4), 441−444.
(4) Umeda, T.; Tsuzuki, S. *Adsorption Characteristics of Lithography Filters in Various Solvents Using Application-Specific Ratings*; SPIE, 2014; Vol. *9051*, pp 358−365.
(5) Umeda, T.; Shiu, E.; Mizuno, T.; Nakagawa, H.; Murakami, T.; Tsuzuki, S. *Start-up Performance and Pattern Defectivity Improvement Using 2nm Rated Nylon Filter Developed with Lithography Filtration Expertise*; SPIE, 2019; Vol. *10960*, pp 144−150.
(6) Varanasi, R.; Mesawich, M.; Connor, P.; Johnson, L. Advanced Lithographic Filtration and Contamination Control for 14nm Node and beyond Semiconductor Processes. *Proc. SPIE* **2017**, *10146*, 202462B.
(7) Gorodokin, V.; Zemlyanov, D. Metallic Contamination in Silicon Processing. In *Proceedings of the 2004 23rd IEEE Convention of Electrical and Electronics Engineers in Israel*; IEEE, 2004; pp 157−160. .
(8) Hsiao, C.-J.; Teng, A.-S.; Chang, W.-C.; Chen, Y.-Y.; Lee, M.-Y.; Tsai, Y.-S.; Lee, T.-W.; Lin, D.-J.; Dai, A.; Lu, C.-Y. Investigation of Chromium Contamination Induced TDDB Degradation in MOSFET. In *Proceedings of the 20th IEEE International Symposium on the Physical and Failure Analysis of Integrated Circuits (IPFA)*; IEEE, 2013; pp 61−64.
(9) Chen, C.-H.; Tsai, H.-J.; Huang, K.-S.; Liu, H.-T. *Study for Cross Contamination between Cmos Image Sensor and IC Product*; IEEE, 2001; pp 121−123.
(10) Fernández-Olmo, I.; Fernández, J. L.; Irabien, A. Purification of Dilute Hydrofluoric Acid by Commercial Ion Exchange Resins. *Sep. Purif. Technol.* **2007**, *56* (1), 118−125.
(11) Krivan, V.; Koch, B. Determination of Ca, Cu, Fe, K, Na, and Si in Polyimides for Microelectronics by Electrothermal Atomic Absorption Spectrometry Involving Sample Dissolution in Organic Solvents. *Anal. Chem.* **1995**, *67* (18), 3148−3153.
(12) Wu, A.; Kohyama, T.; Hamzik, J.; Ly, S.; Jaber, J. *Targeted Removal of Metallic Contamination from Lithography Solvents Using Membrane Purifiers*; SPIE, 2018; Vol. *10586*, pp 138−148.
(13) Fernández-Olmo, I.; Fernández, J. L.; Irabien, A. Purification of Dilute Hydrofluoric Acid by Commercial Ion Exchange Resins. *Sep. Purif. Technol.* **2007**, *56* (1), 118−125.
(14) Hussain, A.; Chaniago, Y. D.; Riaz, A.; Lee, M. Process Design Alternatives for Producing Ultra-High-Purity Electronic-Grade Propylene Glycol Monomethyl Ether Acetate. *Ind. Eng. Chem. Res.* **2019**, *58* (6), 2246−2257.
(15) Kim, H.-B.; Ueno, K.; Chiba, M.; Kogi, O.; Kitamura, N. Spatially-Resolved Fluorescence Spectroscopic Study on Liquid/Liquid Extraction Processes in Polymer Microchannels. *Anal. Sci.* **2000**, *16* (8), 871−876.
(16) Yamamoto, K.; Shimono, T.; Okada, T.; Kawazawa, Y.; Tatsuno, T. New Method of Purification of HF Chemicals for Very Large Scale Integration Manufacturing. *J. Electrochem. Soc.* **1996**, *143* (12), 4119−4124.
(17) Entezarian, M.; Geiger, B. *The Effect of Materials Selection on Metals Reduction in Propylene Glycol Methyl Ether Acetate*; PGMEA; SPIE, 2016; Vol. *9778*, pp 1079−1084.
(18) Efome, J. E.; Rana, D.; Matsuura, T.; Lan, C. Q. Insight Studies on Metal-Organic Framework Nanofibrous Membrane Adsorption and Activation for Heavy Metal Ions Removal from Aqueous Solution. *ACS Appl. Mater. Interfaces* **2018**, *10* (22), 18619−18629.
(19) Shahzad, F.; Alhabeb, M.; Hatter, C. B.; Anasori, B.; Man Hong, S.; Koo, C. M.; Gogotsi, Y. Electromagnetic Interference Shielding with 2D Transition Metal Carbides (MXenes). *Science* **2016**, *353* (6304), 1137−1140.
(20) Xie, X.; Chen, C.; Zhang, N.; Tang, Z.-R.; Jiang, J.; Xu, Y.-J. Microstructure and Surface Control of MXene Films for Water Purification. *Nat. Sustain.* **2019**, *2* (9), 856−862.
(21) Othman, Z.; Mackey, H. R.; Mahmoud, K. A. A Critical Overview of MXenes Adsorption Behavior toward Heavy Metals. *Chemosphere* **2022**, *295*, 133849.
(22) Er, D.; Li, J.; Naguib, M.; Gogotsi, Y.; Shenoy, V. B. Ti3C2MXene as a High Capacity Electrode Material for Metal (Li, Na, K, Ca) Ion Batteries. *ACS Appl. Mater. Interfaces* **2014**, *6* (14), 11173−11179.
(23) Rana, D.; Mandal, B.; Bhattacharyya, S. Analogue Calorimetric Studies of Blends of Poly (Vinyl Ester) s and Polyacrylates. *Macromolecules* **1996**, *29* (5), 1579−1583.
(24) Naguib, M.; Kurtoglu, M.; Presser, V.; Lu, J.; Niu, J.; Heon, M.; Hultman, L.; Gogotsi, Y.; Barsoum, M. W. Two-dimensional Nanocrystals Produced by Exfoliation of Ti3AlC2. *Adv. Mater.* **2011**, *23* (37), 4248−4253.
(25) Shuck, C. E.; Sarycheva, A.; Anayee, M.; Levitt, A.; Zhu, Y.; Uzun, S.; Balitskiy, V.; Zahorodna, V.; Gogotsi, O.; Gogotsi, Y. Scalable Synthesis of Ti3C2Tx Mxene. *Adv. Eng. Mater.* **2020**, *22* (3), 1901241.
(26) Ren, C. E.; Hatzell, K. B.; Alhabeb, M.; Ling, Z.; Mahmoud, K. A.; Gogotsi, Y. Charge- and Size-Selective Ion Sieving Through Ti3C2Tx MXene Membranes. *J. Phys. Chem. Lett.* **2015**, *6* (20), 4026−4031.

(27) Nightingale, E., Jr Phenomenological Theory of Ion Solvation. Effective Radii of Hydrated Ions. *J. Phys. Chem.* **1959**, *63* (9), 1381−1387.
(28) Ying, Y.; Liu, Y.; Wang, X.; Mao, Y.; Cao, W.; Hu, P.; Peng, X. Two-Dimensional Titanium Carbide for Efficiently Reductive Removal of Highly Toxic Chromium(VI) from Water. *ACS Appl. Mater. Interfaces* **2015**, *7* (3), 1795−1803.
(29) Riazi, H.; Anayee, M.; Hantanasirisakul, K.; Shamsabadi, A. A.; Anasori, B.; Gogotsi, Y.; Soroush, M. Surface Modification of a MXene by an Aminosilane Coupling Agent. *Adv. Mater. Interfaces* **2020**, *7* (6), 1902008.
(30) Alhabeb, M.; Maleski, K.; Anasori, B.; Lelyukh, P.; Clark, L.; Sin, S.; Gogotsi, Y. Guidelines for Synthesis and Processing of Two-Dimensional Titanium Carbide (Ti3C2T x MXene). *Chem. Mater.* **2017**, *29* (18), 7633−7644.

https://doi.org/10.1021/acsaenm.3c00450
ACS Appl. Eng. Mater. 2023, 1, 2452−2457